Numerical Analysis on Entire Temperature Field of Horseshoe-shaped Tunnel Fire

Mingzhe Sun[1],Guoqing Zhu[1*],Yunji Gao[1,2]

[1]*School of Safety Engineering, China University of Mining and Technology, Xuzhou Jiangsu 221116, P.R. China*
[2]*Fire Fighting and Rescue Technology Key Laboratory of MPS, Langfang, Hebei, 065000, PR China*
Corresponding author e-mail: zgq119xz@cumt.edu.cn

Keywords: Tunnel fire; temperature field; transverse distribution; longitudinal attenuation.

Abstract: FDS (Fire Dynamics Simulator) is used to simulate different HRRs fires in a horseshoe-shaped tunnel model with a real cross-sectional size of 1:1. Thermocouples are arranged in different cross sections of the tunnel to obtain entire temperature field. The ceiling maximum temperature prediction formula and the ceiling longitudinal temperature attenuation prediction formula are obtained which are consistent with the model of Albert and Gong. It is found that the dimensionless transverse temperature rise distribution under the semicircular ceiling conforms to Boltzmann curve, but the coefficients of the fitting formula are different in the turbulent flow zone near the fire source and the laminar flow zone away from the fire source. Transverse temperature distribution at the sidewall can be regarded as constant which equal to the temperature at the button of semicircular ceiling in most engineering applications. A prediction model is established to estimate the temperature of each position of tunnel wall. It provides a more accurate and detailed temperature field prediction method for tunnel fire prevention and structural damage research.

1. Introduction

Tunnel fire caused a lots of major accidents due to its highly dangerous characteristic [1]. For example, subway fires in Baku, the capital of Azerbaijan, and Daegu, South Korea, have caused hundreds of deaths and serious damage to the tunnel structure [2]. These major fire accidents have attracted a lot of attention to tunnel fires. Since the high temperature caused by large heat release rate in tunnel fire is the main factor that damages tunnel structure and causes casualties, it is necessary to study the tunnel fire temperature distribution for tunnel fire prevention [3,4].

The maximum temperature under the ceiling of tunnel has been studied wildly. In 1972, Alpert firstly proposed that the maximum temperature rise of the unconfined ceiling is proportional to $2/3$ of the dimensionless heat release rate, and inversely proportional to $-5/3$ of the distance between

the fire source and ceiling [5]. Experiments with different conditions were conducted by other scholars. These results conformed with the conclusions of Alpert, and empirical formulas are obtained with their respective corrections [6,7,8]. As experimental conditions changed, the slope of empirical formula changed accordingly. For example, Tang [9] obtained an empirical formula related to wind speed and fire source aspect ratio by changing the shape of the fire source and the tunnel ventilation rate in a small-scale model. Factors such as top shaft [10], transverse fire location [11] and the inclined angle of tunnel [12] were also considered to have effects on the maximum temperature under ceiling, which were studied respectively.

As for temperature distribution, the longitudinal temperature distribution under the ceiling of tunnel fire has been extensively studied by some scholars. Based on experimental research, Evers [13] proposed a prediction model for the longitudinal temperature attenuation under the ceiling. Gong [14] provided a longitudinal smoke temperature distribution formula that takes into account ambient temperature by theoretical and experimental analysis. Liu [15] studied the effect of tunnel section coefficient on longitudinal temperature distribution by a series of small-scale model experiments. Shota [16] studied the effect of exhaust shaft on the longitudinal temperature distribution of tunnel by changing size and aspect ratio of the exhaust shaft at the top of tunnel. Li [17] conducted a series of experiments to study the influence of longitudinal ventilation on the longitudinal temperature attenuation.

At present, there are few studies on the transverse temperature distribution of tunnel fire. Fan [18] studied the influence of the distance between fire source and side wall on ceiling transverse temperature distribution by a small-scale model with a length of 6 m, and proposed a model based on Alpert's empirical formula to predict the transverse temperature distribution of different cross sections. Gao [19] presented an experimental investigation on the transverse ceiling flame length and the temperature distribution of a sidewall confined tunnel model. The ceiling transverse temperature distribution is divided into three parts: continuous flame zone, intermittent flame zone and buoyancy plume zone, which can be predicted by different equations respectively.

Previous studies were based on simplify small-scale models with rectangular cross section.The longitudinal temperature studies can only predict the longitudinal temperature attenuation on the straight line under ceiling which centered on the fire source. Rare transverse temperature distribution studies are limited to the temperature under horizontal ceiling, lacking curved ceiling and sidewall of tunnel. A model for predicting the entire temperature field of tunnel fire has not been extensively studied. In fact, the temperature rise caused by the influence of heat radiation and convection on the sidewall of tunnel is also an important factor for the structural stability damage in tunnel fire. Therefore, it is necessary to study the entire temperature field of the tunnel fire.

In this paper, the 1:1 horseshoe-shaped concrete tunnel model is established with FDS software, and the longitudinal and transverse temperature distribution of the semicircular ceiling and the vertical sidewall are explored respectively to obtain the empirical formula for predicting the entire temperature field of tunnel. This research can provide detailed temperature field data for the study of tunnel structures in fire.

2. Experimental Setup

The horseshoe-shaped tunnel is made of concrete with a length of 100 m. The cross section of tunnel with an actual size are shown in Figure 1. It consists of a semicircular ceiling with a radius of 4.4 m and two vertical walls with a height of 3.5 m. The square fire source is placed at the center of the tunnel with a side length of 2 m and a height of 1 m. The heat release rate (HRR) of fire source is set as 8 MW, 14 MW, 20 MW, 26 MW and 32 MW, on the basis of the NFPA 502 (carriage:5 MW, multiple cars:15 MW, bus:30 MW). In order to obtain the entire temperature distribution in the tunnel, temperature measurement sections are arranged every 5 m starting from the fire source position. 31 thermocouples are arranged on every cross section, wherein a thermocouple is placed every 10 ° under the semicircular ceiling. The side wall is placed with 6 thermocouples from a height of 1.2 m to 3.2 m with 0.4 m interval. The grid size is set as 0.25 m*0.25 m*0.25 m, the initial ambient temperature is set as 20 °C, and the HRR is constant.
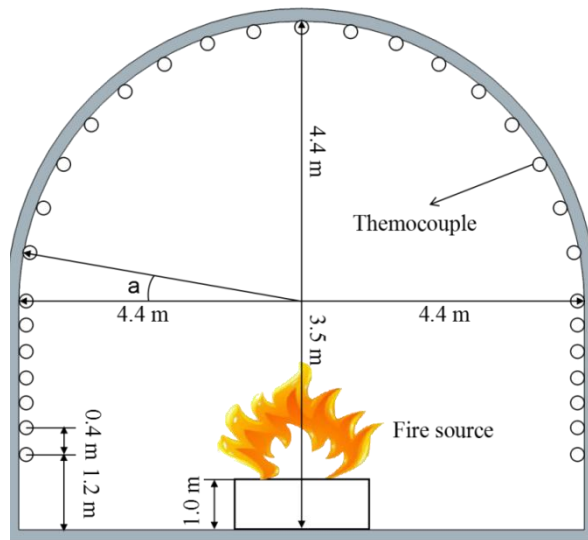
Figure 1: Tunnel cross section.

3. Results and Discussion

3.1 Maximum Temperature Prediction

Since the HRRs of fire source are set as constant, the temperature reaches a steady state after a rapid rise. This phenomenon exists at other thermocouples, but it will have a longer growth stage as the distance from fire source. The long-term tunnel temperature distribution under steady state is the main target of this research, as a result the average temperature of each thermocouple in steady state is taken as the research data. As the tunnel model is completely symmetrical about the fire source, the temperature of the two thermocouples in the corresponding positions under steady state is averaged as the maximum temperature at these positions.

Alpert firstly proposed empirical formula for the maximum temperature rise of unconfined ceiling smoke, as shown in Eq.(1).

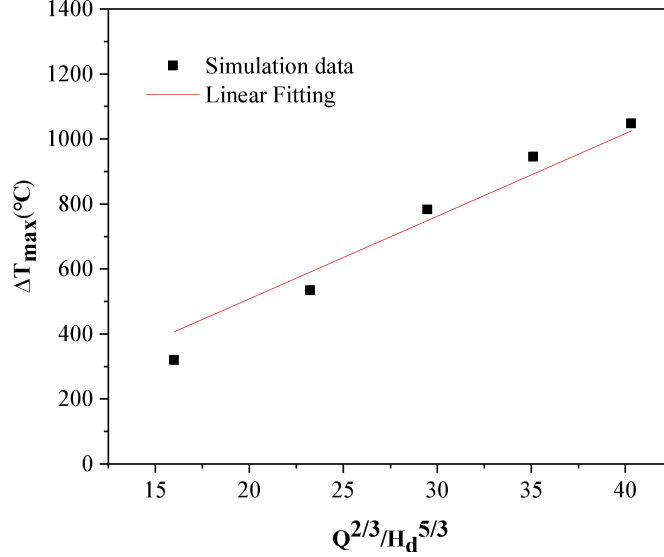$$\Delta T_{\max} = 16.9 \frac{Q^{2/3}}{H_d^{5/3}} \tag{1}$$

Figure 2: Fitting line of maximum temperature rise under different HRRs.

According to previous studies, the slopes of the empirical formula are vary with different experimental conditions. In order to obtain the empirical formula in the case of the tunnel section in this paper, HRR (Q) and the height distance between fire source and the highest of ceiling (H_d) are dimensionless by $Q^{2/3}/H_d^{5/3}$. The maximum temperature rise of the ceiling ($\Delta T_{\max}$) under different HRRs is shown in Figure 2, which can be fitted by Eq.(2). Because of that heat and smoke are confined by semicircular ceiling, the coefficient of Eq.(2) is greater than Eq.(1). The R-Square value of the fitting line is 0.989, which indicates that the simulation is numerically in line with the actual situation.

$$\Delta T_{\max} = 25.4 \frac{Q^{2/3}}{H_d^{5/3}} \tag{2}$$

3.2 Longitudinal Temperature Attenuation

Temperature rise as a function of longitudinal distance (L) from fire source under different HRRs is shown in the Figure 3. It can be observed that there are similar trends under different HRRs: (1) The temperature rise decreases sharply near the fire source and then gets slower as the distance from the fire source. (2) At the same longitudinal position, the temperature rise increases as the HRR.
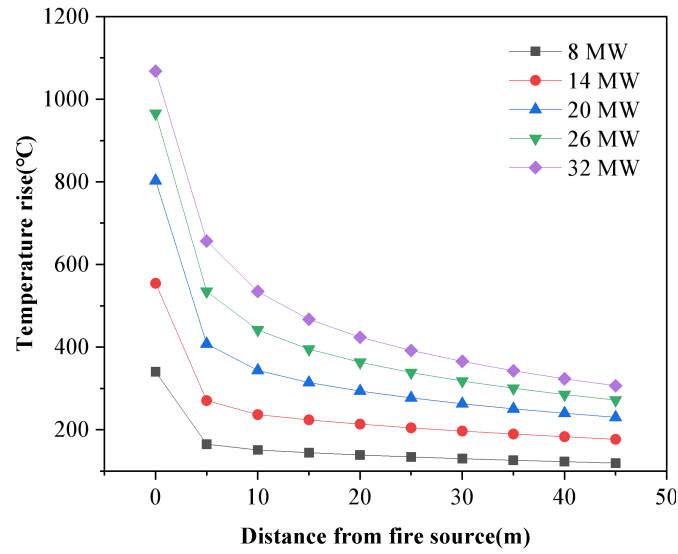
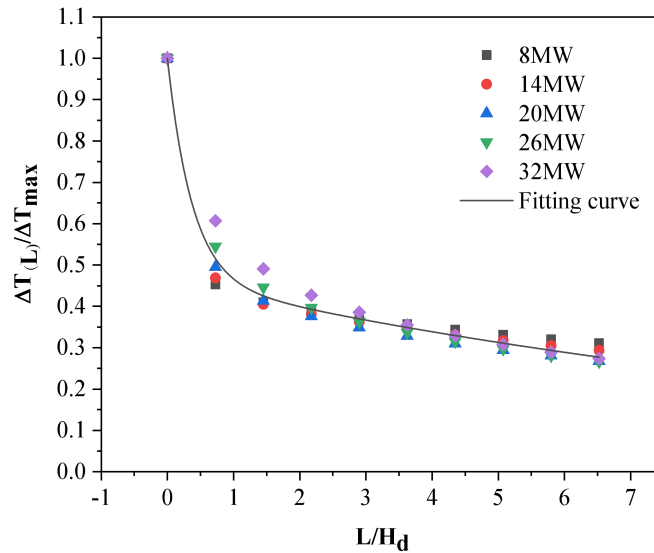Figure 3: Temperature rise as a function of longitudinal distance from fire source under different HRRs.

Figure 4: Dimensionless longitudinal temperature rise as a function of dimensionless distance from fire source under different HRRs.

Table 1: Fitting results of different formulas.

Cases	Evers's formula	R^2	Gong's formula	R^2
Fitting Curve	$\dfrac{\Delta T_{(L)}}{\Delta T_{\max}} = 0.775e^{-0.220L/H_d}$	0.702	$\dfrac{\Delta T_{(L)}}{\Delta T_{\max}} = 0.465e^{-0.079L/H} + 0.534e^{-2.679L/H_d}$	0.986

According to previous studies, the dimensionless temperature rise is exponentially related to the dimensionless longitudinal distance from the fire source. The temperature rise and the longitudinal distance are dimensionless by $\Delta T_{(L)}/\Delta T_{\max}$ (where $\Delta T_{(L)}$ is the temperature rise at distance L from fire source) and L/H_d, whose relationship is shown in Figure 4. To demonstrate the accuracy of the simulated data, Evers and Gong's prediction formulas are used to fit the dimensionless parameters

and their fitting results are shown in Table 1. It can be seen that the R-Square value of Gong's formula (0.986) is much larger than Evers' formula (0.702). The relatively closed long tunnel simulation model and the hot smoke confined by semicircular ceiling cause the ambient air to be heated up rapidly. Therefore, Gong's model is more suitable in this simulation for taking into account ambient temperature.
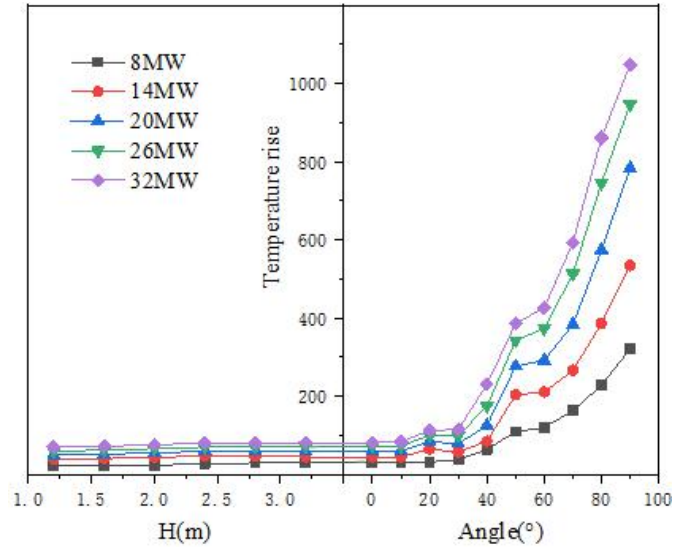
3.3 Transverse Distribution

Figure 5: Transverse temperature rise as a function of Height (H) and Angle (a) at the position of fire source (L=0 m) under different HRRs

The tunnel transverse temperature distribution is divided into two parts: vertical sidewall temperature distribution and semicircular ceiling temperature distribution. The transverse temperature distribution at the location of fire source (L=0) is shown in the Figure5. It can be observed that the temperature rise changes slightly from 1.2 m height of sidewall to a =0˚ (H =3.5 m) of ceiling. The maximum temperature rise span of this zone is 11.3°C when HRR is 32 MW. As the HRR decreases and the distance from the fire source increases, the temperature rise span will decrease to less than 1℃. So transverse temperature distribution at the sidewall can be regarded as constant and equal to the temperature at position where a=0˚ of ceiling in most engineering applications. It can be expressed as Eq.(3)

$$\Delta T_{(H,L)} = \Delta T_{(L,\alpha=0°)} \tag{3}$$

Where $\Delta T_{(H,L)}$ is the temperature rise at the height H from floor of the sidewall at distance L from

fire source. Where $\Delta T_{(L,\alpha=0°)}$ is the temperature rise at the button of ceiling at distance L from fire

source.

For the temperature distribution of the semicircular ceiling when L=0 m, it can be seen from Figure 5: At the position of fire source, the temperature rise rate gradually increases as angle when a=0~40˚. A mutation occurs when a=50~60˚, where rise rate decreases suddenly. Then the

temperature rise continues to increase at a high speed. Similar phenomenon is observed at other position under different HRRs.
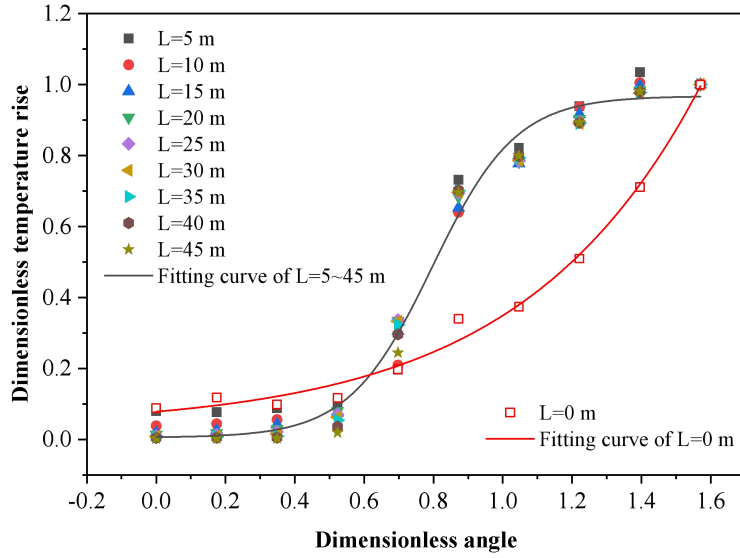

Figure 6: Dimensionless temperature rise as a function of dimensionless angle when HRR is 32 MW.

Table 2: Values of fitting curve.

HRR	Distance from fire source	Values of fitting curve				
		A_1	A_2	θ_0	$d\theta$	R^2
8 MW	0 m	0.035	34.825	3.357	0.501	0.992
	5~45 m	0.005	0.967	0.797	0.120	0.989
14 MW	0 m	0.001	38.802	3.529	0.537	0.982
	5~45 m	0.010	0.971	0.827	0.131	0.989
20 MW	0 m	0.010	14.902	2.898	0.502	0.981
	5~45 m	0.011	0.979	0.855	0.142	0.989
26 MW	0 m	0.028	2.224	1.659	0.393	0.986
	5~45 m	0.018	0.981	0.869	0.146	0.988
32 MW	0 m	0.032	1.909	1.540	0.379	0.991
	5~45 m	0.022	0.985	0.879	0.150	0.988
8~32 MW	0 m	0.022	4.025	2.088	0.459	0.986
	5~45 m	0.013	0.976	0.844	0.139	0.986

In order to study the temperature distribution of the ceiling, the temperature rise and angle are dimensionless by $\Delta T_{(\theta)} / \Delta T_{(L)}$ (where $\Delta T_{(\theta)}$ is the temperature rise at the position of ceiling whose dimensionless angle is θ) and $\theta = \pi a / 180°$,whose relationship is shown in the Figure 6 (HRR is 32 MW). The fitting curve of temperature rise of the cross section at the position of fire source is monotonous, and the slope is larger as dimensionless angle. While the fitting curve of the cross section away from fire source is s-shaped, the slope gradually increases at first and then decreases. This phenomenon is consistent with the results of Gao's research: transverse temperature of the turbulent zone near the fire source has a different distribution trend from the laminar zone away from the fire source. In this paper, these trends can be fitted by Boltzmann formula which is shown

in Eq.(4). Given the similar trends observed and similar values of fitting formulas under different HRRs, dimensionless transverse temperature rise under different HRRs can be fitted by two fitting curves. The above values of fitting formulas are simulated in Table 2.

$$\frac{\Delta T_{(\theta)}}{\Delta T_{(L)}} = A_2 + \frac{A_1 - A_2}{1 + e^{\frac{\theta - \theta_0}{d\theta}}} \tag{4}$$

Due to the high R-Square values of the fitting curves in turbulent zone and laminar zone, a prediction model of the transverse temperature distribution of the ceiling under different HRRs is obtained. The formula for predicting the temperature rise at the position of fire source is shown as Eq.(5)

$$\frac{\Delta T_{(\theta)}}{\Delta T_{\max}} = 4.025 + \frac{0.022 - 4.025}{1 + e^{\frac{\theta - 2.088}{0.459}}} \ (L = 0 \ m) \tag{5}$$

The formula for laminar zone is shown as Eq.(6)

$$\frac{\Delta T_{(\theta)}}{\Delta T_{(L)}} = 0.976 + \frac{0.013 - 0.976}{1 + e^{\frac{\theta - 0.844}{0.139}}} \ (L \geq 5 \ m) \tag{6}$$

According to Eq.(5) and Eq.(6), the entire temperature field of the ceiling can be predicted. Merging Eq.(3) with Eq.(5) and Eq.(6) when θ=0, respectively. The temperature prediction formulas at the side wall are also obtained as shown in Eq.(7) and Eq.(8).

$$\Delta T_{(H)} = 0.064 \Delta T_{\max} \ (L = 0 \ m) \tag{7}$$

$$\Delta T_{(H,L)} = 0.015 \Delta T_{(L)} \ (L \geq 5 \ m) \tag{8}$$

By correcting formula Eq.(2) from the Alpert's model, the maximum temperature under the ceiling of tunnel fire can be predicted by HRR and the height between ceiling and fire source. Based on this maximum temperature prediction, by correcting the formula from the Gong's model, the longitudinal temperature attenuation at the highest positions of the tunnel can be predicted. In this paper, the empirical formulas for transverse temperature distribution by the temperature at the highest position of ceiling are obtained. Merging the formulas of Gong and Eq.(2),(5),(6),(7),(8) to obtain the temperature distribution at each position of tunnel by the HRR of fire source and the distance between the ceiling and fire source. These formulas are shown in Eq.(9),(10),(11) and (12).

$$\Delta T_{(\theta)} = 25.4(4.025 + \frac{0.022 - 4.025}{1 + e^{\frac{\theta - 2.088}{0.459}}}) \frac{Q^{2/3}}{H_d^{5/3}} \ (L = 0 \ m) \tag{9}$$

$$\Delta T_{(H)} = 1.626 \frac{Q^{2/3}}{H_d^{5/3}} \ (L = 0 \ m) \tag{10}$$

$$\Delta T_{(\theta,L)} = 25.4(0.976 + \frac{0.013 - 0.976}{1 + e^{\frac{\theta - 0.844}{0.139}}})(0.465 e^{-0.079 \frac{L}{H_d}} + 0.534 e^{-2.679 \frac{L}{H_d}}) \frac{\dot{Q}^{2/3}}{H_d^{5/3}} (L \geq 5 \ m) \tag{11}$$

$$\Delta T_{(H,L)} = 0.381(0.465 e^{-0.079 \frac{L}{H_d}} + 0.534 e^{-2.679 \frac{L}{H_d}}) \frac{\dot{Q}^{2/3}}{H_d^{5/3}} \ (L \geq 5 m) \tag{12}$$
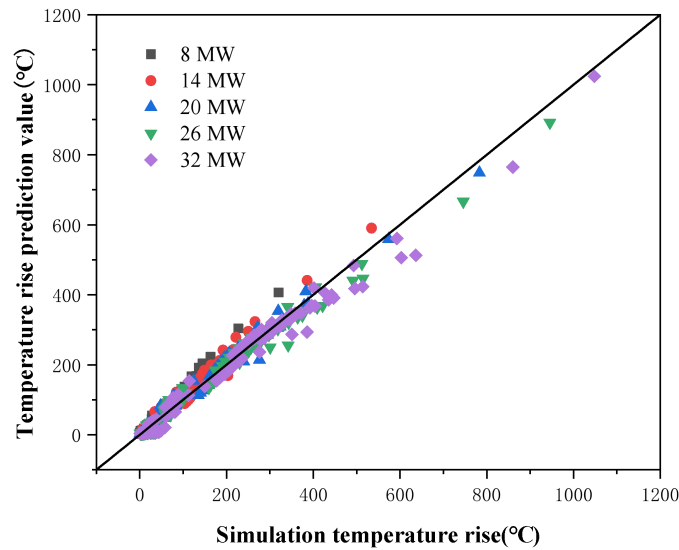
Figure 7: Comparison of the entire temperature filed values predicted by Eq.(9),(10),(11) and (12)with the simulation values under different HRRs.

The comparison of entire temperature filed values predicted by Eq.(9),(10),(11) and(12) with the simulation values are shown in the Figure 7. It can be observed that the model effectively predict the entire temperature distribution with different HRRs and distance between fire source and ceiling. These predictions are sufficient for engineering applications. In fact, for the temperature distribution near the fire source (L<5 m) which is not taken account of in this prediction model, the conservative prediction results can be obtained by directly using the laminar flow region prediction formula (11) and (12). This is due to the fitting curve of laminar zone is mostly higher than the turbulent zone at the fire source location, as the distance increases, the fitting curve of turbulent zone will gradually change to be consistent with the curve of laminar zone. While more accurate prediction of turbulent zone still need to be further studied.

4. Conclusions

The formulas which can predict the maximum temperature under the ceiling and the longitudinal temperature attenuation at the highest position of ceiling are obtained. This proves that it is not accurate to consider the ambient temperature as a constant value in an approximately closed tunnel fire.

(2) Under the HRRs of 8-32 MW, the temperature distribution on sidewall at the same distance of fire source change slightly (<11.3 °C). Transverse temperature distribution on the sidewall can be regarded as constant and equal to the temperature at position where a=0° of ceiling in most engineering applications.

(3) It is found that there are some differences between the transverse temperature distribution of the ceiling at the section of fire source (turbulent zone) and the section away from fire source (laminar zone). The prediction formulas with different coefficients are obtained by dimensionless fitting with Boltzmann cure respectively. Combined with the prediction formulas for maximum temperature and longitudinal temperature attenuation, A new method is proposed to predict the

entire temperature distribution of the tunnel fire by the heat release rate and the height between the ceiling and fire source.

Acknowledgments

References

[1] Bendelius, A. G. . (2002). Tunnel fire and life safety within the world road association (piarc). Tunnelling & Underground Space Technology Incorporating Trenchless Technology Research, 17(2), 159-161.

[2] Zhao, H. L. , Xu, Z. S. , & Jiang, X. P. . (2010). Reduced-scale model tests of fires in railway tunnel and structure fire safety. Advanced Materials Research, 168-170, 2473-2476.

[3] Mcgrattan, K. , & Hamins, A. . (2006). Numerical simulation of the howard street tunnel fire. Fire Technology, 42(4), 273-281.

[4] Ingason, H. , Li, Y. Z. , & Lönnermark, Anders. (2015). Tunnel fire dynamics. Springer.

[5] Alpert, R. L. . (1972). Calculation of response time of ceiling-mounted fire detectors. Fire Technology.

[6] Li, Y. Z. , & Ingason, H. . (2012). The maximum ceiling gas temperature in a large tunnel fire. Fire Safety Journal, 48(none), 38-48.

[7] Yongzheng, Y. , Kun, H. , Min, P. , Long, S. , Xudong, C. , & Heping, Z. . (2018). Maximum gas temperature rise beneath the ceiling in a portals-sealed tunnel fire. Tunnelling and Underground Space Technology, 80, 10-15.

[8] Li, Y. Z. , Lei, B. , & Ingason, H. . (2011). The maximum temperature of buoyancy-driven smoke flow beneath the ceiling in tunnel fires. Fire Safety Journal, 46(4), 204-210.

[9] Tang, F. , Cao, Z. , Palacios, A. , & Wang, Q. . (2018). A study on the maximum temperature of ceiling jet induced by rectangular-source fires in a tunnel using ceiling smoke extraction. International Journal of Thermal Sciences, 127, 329-334.

[10] Wang, Y. F. , Li, Y. L. , Yan, P. N. , Zhang, B. , Jiang, J. C. , & Zhang, L. .(2015). Maximum temperature of smoke beneath ceiling in tunnel fire with vertical shafts. Tunnelling and Underground Space Technology, 50, 189-198.

[11] Ji, J. , Fan, C. G. , Zhong, W. , Shen, X. B. , & Sun, J. H. . (2012). Experimental investigation on influence of different transverse fire locations on maximum smoke temperature under the tunnel ceiling. International Journal of Heat and Mass Transfer, 55(17-18), 4817-4826.

[12] Ji, J. , Wan H. X. , Li, K. Y. , Han, J. Y. , & Sun, J. H. . (2015). A numerical study on upstream maximum temperature in inclined urban road tunnel fires. International Journal of Heat and Mass Transfer, 88, 516-526.

[13] Evers E, Waterhouse A (1981) A complete model for analyzing smoke movement in building.

[14] Gong L, Jiang L, Li S, Shen N, Zhang Y, Sun J (2016) Theoretical and experimental study on longitudinal smoke temperature distribution in tunnel fires. International Journal of Thermal Sciences 102:319-328. doi:10.1016/j.ijthermalsci.2015.12.006

[15] Liu, F. , Yu, L. X. , Weng, M. C. , & Lu, X. L. . (2016). Study on longitudinal temperature distribution of fire-induced ceiling flow in tunnels with different sectional coefficients. Tunnelling and Underground Space Technology incorporating Trenchless Technology Research, 54, 49-60.

[16] Shota, T. , Futoshi, T. , Kazuhiro, Y. , & Moinuddin, K. A. M. . (2018). Effects of scale ratio and aspect ratio in predicting the longitudinal smoke-temperature distribution during a fire in a road tunnel with vertical shafts. Tunnelling and Underground Space Technology, 80, 78-91.

[17] Li, L. , Li, S. , Wang, X. , & Zhang, H. . (2012). Fire-induced flow temperature along tunnels with longitudinal ventilation. Tunnelling and Underground Space Technology, 32, 44-51.

[18] Fan, C. G. , Ji, J. , Gao, Z. H. , & Sun, J. H. . (2013). Experimental study on transverse smoke temperature distribution in road tunnel fires. Tunnelling and Underground Space Technology, 37(6), 89-95.

[19] Gao, Z. , Jie, J. , Wan, H. , Zhu, J. , & Sun, J. . (2017). Experimental investigation on transverse ceiling flame length and temperature distribution of sidewall confined tunnel fire. Fire Safety Journal, S0379711217301212.